

Analysis of a mechanism suspension to reduce noise from horizontal vibrating screens^{1),2)}

David S. Yantek^{a)} and M. Jenae Lowe^{b)}

A-weighted sound levels around vibrating screens in coal preparation plants often exceed 90 dB. The National Institute for Occupational Safety and Health (NIOSH) is developing noise controls to reduce noise generated by horizontal vibrating screens. Horizontal vibrating screen noise is dominated by sound radiated from the screen body. NIOSH researchers analyzed a mechanism suspension system that could reduce screen body-radiated noise. A finite element (FE) model of the entire screen was used to analyze the screen with the added mechanism suspension. The spring rates for the mechanism suspension were tuned to transmit vibration at the mechanism operating speed while attenuating vibration transmitted from the mechanisms to the screen body at frequencies above 100 Hz. The FE results were used to estimate the A-weighted sound power level radiated by the screen sides and feedbox for various mechanism suspension spring rates. The results indicate that a tuned mechanism suspension could reduce the A-weighted sound power level radiated by the screen body due to gear and bearing forces inside the mechanisms by 7 to 18 dB.
© 2011 Institute of Noise Control Engineering.

1 INTRODUCTION

In an effort to reduce the occurrence of noise-induced hearing loss in the mining industry, the Mine Safety and Health Administration (MSHA) modified its rules regarding noise exposure in 1999¹. Instead of relying on hearing protection devices, MSHA requires mine operators to use all feasible engineering and/or administrative controls to reduce the noise exposures of miners who are overexposed according to MSHA's Permissible Exposure Level (PEL) criteria—i.e., a 90 dB(A) time-weighted average sound level for an 8-hour workday using a 5-dB exchange rate¹. Despite MSHA's requirement to use noise controls, for many

machines, such as vibrating screens, noise controls that reduce the operator's noise exposure below the MSHA PEL do not exist. In these cases, mine operators must use booths or administrative controls to reduce worker noise exposure.

National Institute for Occupational Safety and Health (NIOSH) data from 1999 to 2004 show that 20 out of 46 coal preparation plant workers had noise exposures that exceeded the MSHA PEL noise dose². MSHA PEL noise doses up to 220% have been recorded for preparation plant workers such as stationary equipment operators, froth cell operators, plant operators, plant controls men, third floor operators, wet plant attendants, sump floor operators, plant backups, and plant mechanics. These job classifications require the worker to spend a significant portion of a shift in the plant while working around slurry pumps, dryers, centrifuges, and vibrating screens.

In the United States, there are 879 coal preparation plants, and 570 of these have been active at some time between 2008 and 2010³. Twenty-four states have active coal preparation plants. West Virginia (22%), Kentucky (22%), and Pennsylvania (19%) have the most coal preparation plants. There were 8,290 coal preparation plant workers in 2008 and 8,343 in 2009. According to MSHA data, 1,170 noise-related injuries

¹⁾ This is the first paper published in NCEJ on the special topic of Noise in Mines.

²⁾ The findings and conclusions in this report have not been formally disseminated by the National Institute for Occupational Safety and Health and should not be construed to represent any agency determination or policy. Reference to specific brand names does not imply endorsement by NIOSH.

^{a)} NIOSH, 626 Cochran Mill Rd, P.O.Box 18070, Pittsburgh, PA 15236; email: DYantek@cdc.gov.

^{b)} NIOSH, 626 Cochran Mill Rd, P.O.Box 18070, Pittsburgh, PA 15236; email: MLowe@cdc.gov.

have been reported in mining since 2000. Three hundred fifty-five of these cases (30% of all noise-related injuries) involve preparation plant employees³.

Vibrating screens generate A-weighted sound levels from 90 to 95 dB during clean bituminous coal processing, and from 95 to 100 dB during refuse and anthracite processing⁴. Since screens are used to size, separate, and dewater both coal and refuse (rock) of various sizes, they may be located on many floors within a preparation plant. The number of screens in a processing plant can range from a single screen to more than a dozen. Consequently, preparation plant workers can be exposed to high sound levels generated by screens many times during a workday. Vibrating screens are a major noise problem in coal preparation plants because screens are used extensively in the plants, are usually located in high traffic areas, and can generate high sound levels⁵.

A horizontal vibrating screen (see Fig. 1) is a large machine used to process clean coal that has been separated from refuse materials using a water-magnetite mixture. The magnetite is recovered so that it can be reused in the processing plant, and because it lowers the heating value of coal. The screen body has two sides made of steel plates and a screening surface made of steel wire, which is welded to a frame with small gaps between the wires. Round cross-tubes are used at either end of the screen to help stiffen the structure. The screen is supported on a steel coil spring suspension. One or more vibration mechanisms are mounted to a steel beam that connects the sides of the screen. The vibration mechanisms, which use eccentric shafts to generate vibration, are belt-driven by an electric motor. The vibration mechanisms are designed such that forces are applied normal to the top flange of the H-beam, which is rotated 45 degrees from vertical. For the screen that is the focus of this work, the vibration mechanisms are driven at 900 RPM (15 Hz).

When a horizontal vibrating screen is in use, coal flows from a delivery chute into the screen's feedbox, which is made of steel. The screen, which is designed to vibrate on a 45-degree angle, forces the coal particles to travel across its deck under a water spray that washes the magnetite from the coal. The liquid and fine coal particles pass through the gaps in the screening deck as the material flows toward the discharge end of the screen. Finally, the rinsed coal falls off the discharge end of the screen, where it enters another chute for further processing.

Previous NIOSH studies showed that the A-weighted sound levels around a group of eight horizontal vibrating screens used to process clean coal ranged from 94 to 98 dB⁶. A series of measurements in the same preparation plant indicated that noise due to

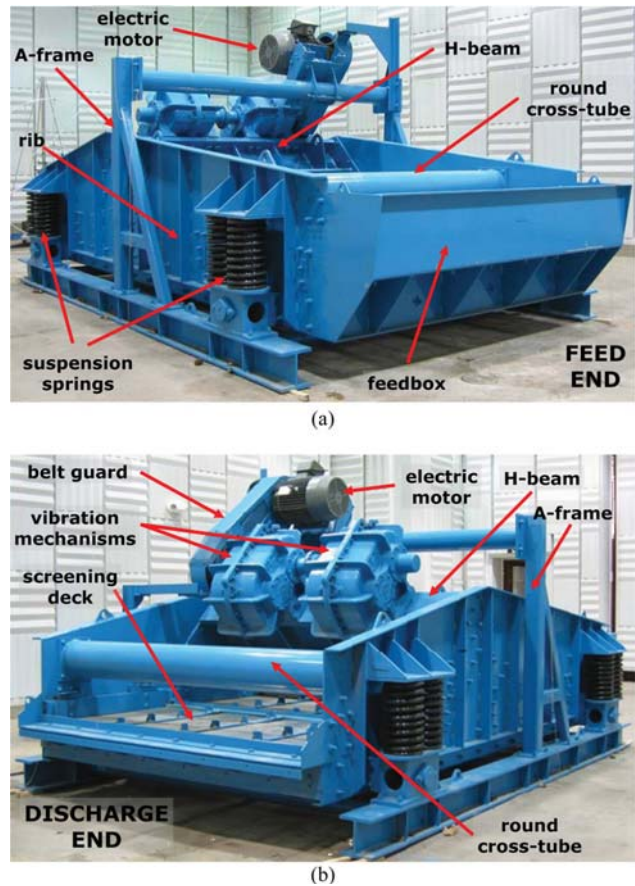


Fig. 1—A horizontal vibrating screen used to process coal viewed from (a) feed end and (b) discharge end.

vibration was the dominant noise source, whereas noise from material flow was less significant. Further research showed that most of the noise due to vibration is radiated by the screen body and the mechanism housings^{7,8}. Screen body noise is the main noise source below about 1 kHz, while mechanism housing noise is the primary source above 1 kHz. The sound energy at frequencies below 1 kHz accounts for about 80% of the overall A-weighted sound power level. In addition, operating deflection shape analysis revealed significant response on the screen sides and feedbox⁹. Noise control efforts were split between developing noise controls to reduce noise above 1 kHz from the mechanism housings and below 1 kHz from the screen body.

To reduce noise above 1 kHz, the NIOSH Office of Mining Safety and Health Research (OMSHR) applied constrained layer damping (CLD) treatments to the mechanism housings and installed an acoustically treated mechanism enclosure¹⁰. Figure 2 shows the 1/3-octave-band sound power level spectra for the baseline, with CLD treatments on the mechanism housings, and with both CLD treatments and an enclosure

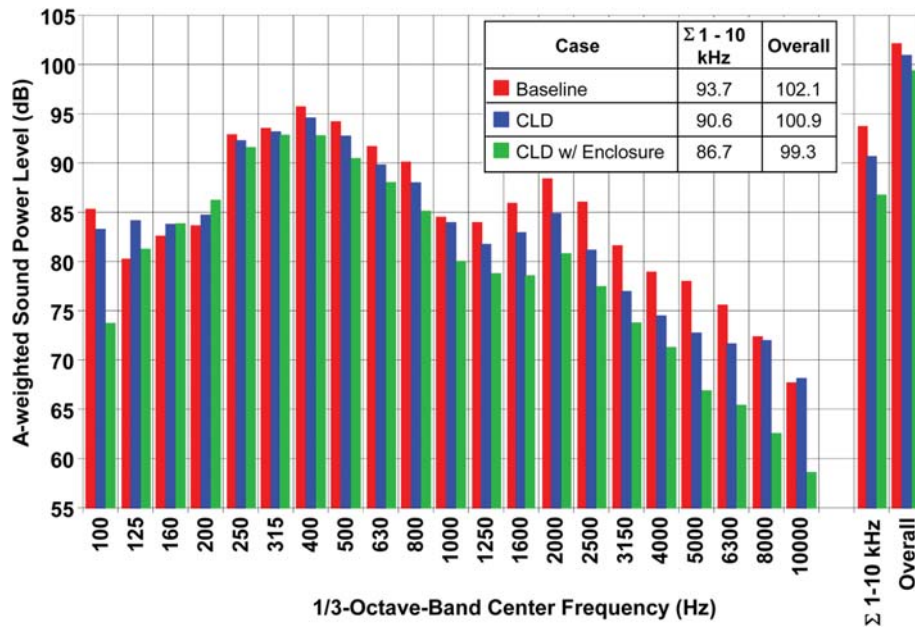


Fig. 2—One-third-octave-band sound power level spectra for the baseline screen, for the screen with CLD treatments on the mechanism housings, and for the screen with CLD treatments and an enclosure applied to the mechanisms.

applied to the mechanisms. In the 1–10 kHz frequency range, which is dominated by mechanism housing noise, the CLD treatments reduced the A-weighted sound power level by 3 dB. In addition, the CLD reduced the overall A-weighted sound power level by 1.2 dB. Adding an enclosure reduced the A-weighted sound power level in the 1–10 kHz frequency range by an additional 3.9 dB and the overall A-weighted sound power level by an additional 2 dB.

In an effort to reduce noise below 1 kHz, the effects of adding stiffeners to the screen sides and feedbox and the effects of increasing its damping were evaluated using an FE model¹¹. The surface-averaged mean-square velocities calculated from the FE results were used with estimated radiation efficiencies to estimate the A-weighted sound power level from the screen sides and feedbox. The study showed that adding stiffeners would have little impact on the sound power level. However, a five-fold increase in the modal damping resulted in a predicted reduction of 7.8 dB.

Due to the screen manufacturer’s concern about the process required to install constrained layer damping treatments, the screen manufacturer was interested in other noise controls that could reduce sound levels below 1 kHz. Vibrating screens are produced using cutting, machining, and welding processes. Because each of these processes generates metal fragments, screen manufacturing plants are not clean enough for the surface preparation and bonding required to make constrained layer damping treatments.

Most screen body noise results from gear noise and bearing chatter within the mechanism housings¹². Clearance within the bearings allows the bearing components to chatter as the machine vibrates. In addition, gear vibrations are transmitted from the mechanism housings to the H-beam. The gear and bearing forces transmitted to the screen could be reduced by adding a suspension between the mechanisms and the H-beam. However, for vibrating screens, the vibratory forces at the mechanism rotation speed must be transmitted to the screen to make it oscillate—thus it can separate coal from refuse and/or products used in coal processing. Given the above constraints, the mechanism suspension system would have to be tuned, so that forces at the mechanism rotation speed are transmitted, while forces at higher frequencies due to gear and bearing forces are attenuated. This tuned mechanism suspension concept to reduce noise emissions below 1 kHz is the focus of this work.

2 MECHANISM SUSPENSION ANALYSIS PROCEDURE

A mechanism suspension is proposed to be added to the screen to reduce noise radiated by the screen body due to gear and bearing forces within the vibration mechanisms. To add a mechanism suspension to the screen, vibration isolators would be inserted between the vibration mechanisms and the H-beam. The

vibration mechanisms would be mounted on top of a large steel plate, or raft. Then, the raft would be mounted on top of the vibration isolators. The goal of adding a mechanism suspension is to separate the primary source of mechanical energy from the noise-radiating structure, but without degrading the performance of the screen.

2.1 Analysis Approach

Prior to designing a mechanism suspension, it is necessary to analyze the dynamic behavior of a screen with an added mechanism suspension. First, a two-degree-of-freedom (DOF) model was used to examine the rigid body behavior of the system. Next, a finite element (FE) model of the screen with an added mechanism suspension was used to examine how the natural frequencies and mode shapes of the system vary with the stiffness of the mechanism suspension. The FE model was then used to perform a forced response analysis on the screen due to forces input at the vibration mechanisms. Finally, the results from the forced response analysis were used to estimate the sound power level radiated by the screen sides and feedbox.

2.2 Two-DOF Model

A simple two-DOF model (see Fig. 3) was used to gain insight into the behavior of a screen with an added

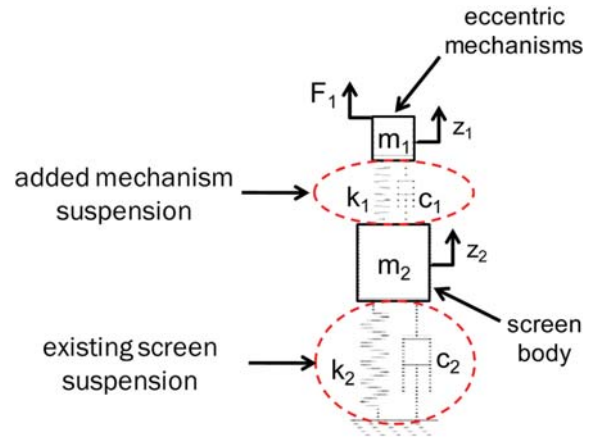


Fig. 3—A simple two-DOF model used to analyze the screen with an added mechanism suspension.

mechanism suspension. In the model, m_2 represents the mass of the screen body and m_1 represents the mass of the vibration mechanisms. The stiffness and damping for the existing screen suspension are represented by k_2 and c_2 , and the stiffness and damping for the mechanism suspension are represented by k_1 and c_1 . The vibration mechanism force is represented by F_1 .

The forced response of the above two-DOF system is given by¹³

$$\begin{bmatrix} z_1(j\omega) \\ z_2(j\omega) \end{bmatrix} = \begin{bmatrix} -m_1\omega^2 + j\omega c_1 + k_1 & -j\omega c_1 - k_1 \\ -j\omega c_1 - k_1 & -m_2\omega^2 + j\omega(c_1 + c_2) + (k_1 + k_2) \end{bmatrix}^{-1} \begin{bmatrix} F_1(j\omega) \\ 0 \end{bmatrix} \quad (1)$$

where ω is the forcing frequency in units of rad/s and j denotes the $\sqrt{-1}$. The force transmitted from the vibration mechanisms to the screen body is

$$F_{mb} = k_1(z_1 - z_2) + c_1(\dot{z}_1 - \dot{z}_2) \quad (2)$$

and the force transmitted from the screen body to the ground is simply

$$F_{bg} = k_2 z_2 + c_2 \dot{z}_2. \quad (3)$$

A computer program was used to solve Eqns. (1), (2), and (3) for a range of mechanism suspension spring rates to examine how the dynamic behavior of the system changes with the mechanism suspension stiffness. The displacement responses for the screen body and the vibration mechanisms, and the forces transmitted from the vibration mechanisms to the screen body and from the screen body to the ground, were examined.

2.3 Finite Element (FE) Model

The two-DOF model can be used to examine the rigid body behavior of the screen with the added mechanism suspension. However, because of the complex structural modes of screens, the two-DOF model is too simplistic and a more complicated model is necessary to analyze the dynamic response of the system. An FE model was developed to analyze the flexible-body dynamic behavior of the screen with an added mechanism suspension (see Fig. 4).

The FE model was based on a previously developed FE model of the screen prior to adding the mechanism suspension¹¹. The first several natural frequencies and mode shapes predicted by the prior model showed good agreement with the first several experimentally determined natural frequencies and mode shapes. In addition, visual comparisons revealed similarities

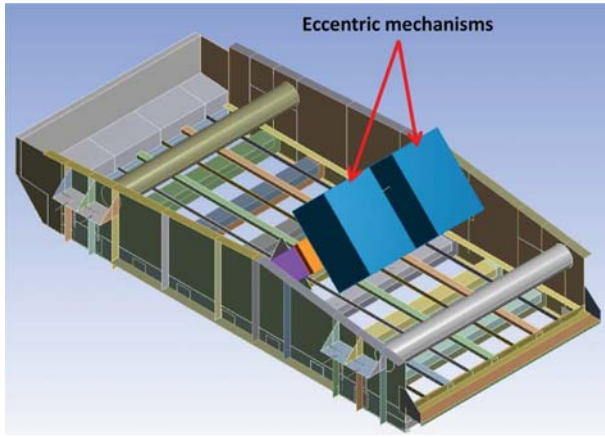


Fig. 4—FE model of the vibrating screen with an added mechanism suspension system.

between experimentally determined operating deflection shapes and the vibration patterns of a forced response analysis with the FE model. In the FE model, the vibration mechanisms were modeled using solid blocks. The density of the blocks was adjusted so that the mass of the blocks matched the mass of the actual mechanisms. The screen deck, which consists of a series of wires with gaps between them, was not included in the model because it would significantly increase its complexity, and because it does not contribute substantially to either the mass or the stiffness of the structure. The A-frame (refer to Fig. 1) used to support the screen was not included because previous tests⁷⁻⁹ showed that it is not a significant noise source. The belt guard was also ignored because it is attached to the A-frame instead of the screen body.

Several simplifications were made to decrease the complexity of the FE model. On the actual screens, the connections between some screen components, such as the ribs and screen sides, are welded joints, whereas the connections between other components, for example the screen sides and round cross-tubes, are bolted joints. In the FE model, all connections were modeled as bonded joints to simplify the model. This approach may overestimate the stiffness and underestimate the damping of the screen. However, the model should still be adequate for comparison purposes. Another simplification used for the model is that the screen suspension springs were modeled using lumped spring elements at each of the mounting locations. Three spring elements were used at each location to model the spring rates in the x-direction (fore/aft), y-direction (vertical), and z-direction (lateral). Each suspension spring was connected to ground with fixed boundary conditions. Steel was used as the material for the entire screen.

To model the addition of a mechanism suspension, the vibration mechanisms were separated from the H-beam by attaching them to a large steel plate, or raft (see Fig. 5). The raft was supported by longitudinal springs with three degrees-of-freedom at six locations. Four of the spring locations were near the corners of the raft, while the remaining two spring locations were at the midpoint of the raft's front and rear edges.

The final FE model had a total of 24,145 nodes and 20,649 solid elements. Because most of the screen is plate-like, shell elements were used to model most of the screen. A total of 19,045 four-node shell elements with six degrees-of-freedom at each node—three translations and three rotations—were used in the model. The remaining 1,604 solid elements were ten-node solid elements with three translational degrees-of-freedom at each node.

The FE model was used to analyze the mechanism suspension in two steps. First, the model was used to solve for the natural frequencies and mode shapes of the screen with the mechanism suspension. The spring rates of the mechanism suspension springs were varied to examine how their stiffness affects the modes. Next, the forced response of the screen was determined for a range of mechanism suspension spring rates. For each case, the displacement responses at 24 points on the screen sides and 15 points on the feedbox were exported for subsequent use when estimating the sound power level radiated from these locations (refer to Fig. 6). The focus was on the sides and feedbox because prior beamforming studies showed that the sides and feedbox were the primary noise-radiating surfaces^{8,9}. In this analysis, a unit load with a flat frequency spectrum from 0 to 500 Hz was applied at each of the vibration mechanisms with a direction spectrum normal to the top of the H-beam. A flat frequency spectrum was

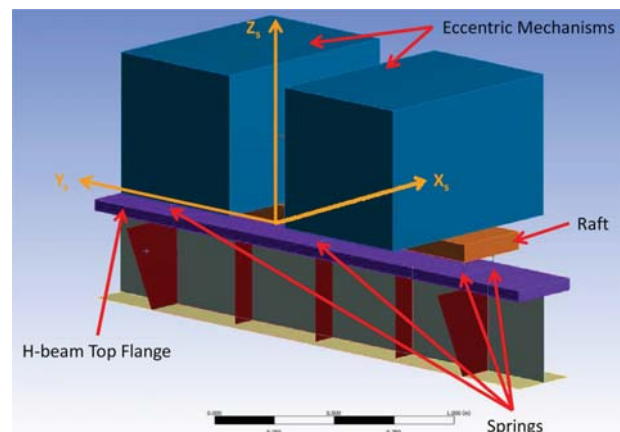


Fig. 5—FE representation of a mechanism suspension consisting of a raft and longitudinal springs.

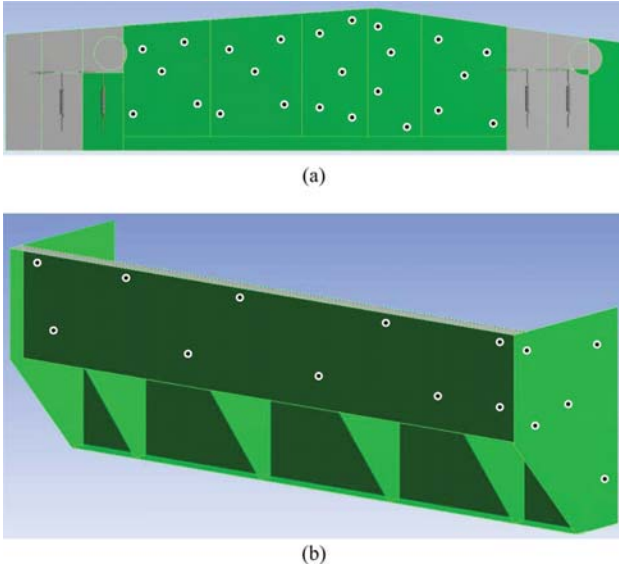


Fig. 6—Point locations used to estimate the sound power level radiated by the (a) screen sides and (b) feedbox.

used to represent the impact forces due to bearing chatter within the vibration mechanisms for simplicity. The analysis was limited to this frequency range because above 500 Hz the modal density was high. The objective of the analysis was to determine the approximate mechanism suspension spring rates needed to reduce the vibration transmitted to and the resulting noise radiated by the screen sides and feedbox.

2.4 Sound Power Level Estimation

The results of the FE model forced response analysis were used to estimate the sound power level radiated by the screen sides and feedbox due to forces from within the vibration mechanisms. For a vibrating object, the sound power level radiated can be estimated by

$$L_W = 10 \log_{10} \langle v \rangle_{s,t}^2 + 10 \log_{10} S + 10 \log_{10} \sigma + 146 \quad (\text{dB re } 10^{-12} \text{W}) \quad (4)$$

where L_W is the sound power level, $\langle v \rangle_{s,t}^2$ is the surface-averaged mean-squared velocity, S is the surface area, and σ is the radiation efficiency¹⁴. Equation (4) was incorporated into a computer program that carried out all calculations for the screen sides and feedbox on a frequency-by-frequency basis in 1 Hz increments. For each set of displacement results, the velocity response at each location was calculated by

$$v = 2\pi f d \quad (5)$$

where d is the displacement magnitude as a function of frequency and f is the excitation frequency in Hz.

The radiation efficiencies of the sides and feedbox were estimated from the thickness and perimeter of each part using data from Bies and Hansen¹⁴. For the screen sides, the areas between stiffening ribs were treated as separate panels (see Fig. 7(a)). The radiation efficiency of each panel was estimated using its perimeter and thickness. For the feedbox, the rear and sides of the feedbox were treated as separate entities (see Fig. 7(b)). The perimeter and thickness of each was used to estimate its radiation efficiency. Within the program, the radiation efficiencies were estimated by curve fitting values from the Bies and Hansen data using a 3rd order polynomial. This provided a simple means of estimating the radiation efficiency on a frequency-by-frequency basis.

Once the radiation efficiencies were estimated, the sound power levels for each panel of the screen sides and for the rear and sides of the feedbox were calculated using Eqn. (4). For the screen sides, the radiation efficiency of each panel was used with its calculated surface-averaged mean-squared velocity. Similarly, for the feedbox, the radiation efficiencies of the rear and sides of the feedbox were used with their calculated surface-averaged mean-squared velocity. The total sound power level for the screen side was calculated by adding the contributions of each panel and the total sound power level for the feedbox was calculated by adding the contributions of the rear and sides of the

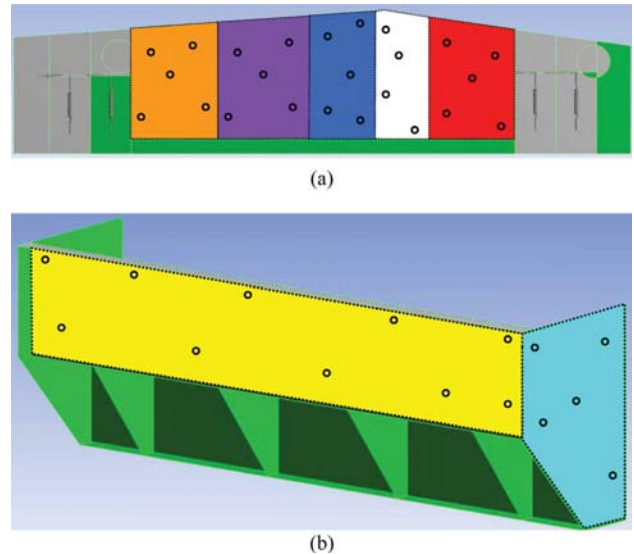


Fig. 7—(a) Individual “panels” used to estimate the sound power level radiated by the screen sides and (b) portions of the feedbox used to estimate the sound power level radiated by the feedbox.

feedbox. In the past, the same approach was applied to examine the sound power level radiated by screens^{9,11}.

Since the MSHA PEL is based on A-weighted sound levels, the program was used to apply A-weighting to the estimated sound power levels. The summation of the sound power levels for the screen sides and feedbox was found by

$$L_{WS+F} = 10\text{LOG}(10^{0.1L_{WS}} + 10^{0.1L_{WF}}) \quad (6)$$

where L_{WS+F} is the estimated sound power level radiated by the sides and feedbox, L_{WS} is the estimated sound power level radiated by the sides, and L_{WF} is the estimated sound power level radiated by the feedbox. For each set of data, the A-weighted 1/3-octave-band sound power level spectrum was computed by summing the narrowband sound power from the lower cutoff frequency to the upper cutoff frequency for each 1/3-octave band. One-third-octave bands were used to simplify the interpretation of the results. Finally, the overall A-weighted sound power level from 0 to 500 Hz was calculated by summing the A-weighted narrowband sound power levels.

3 RESULTS AND DISCUSSION

While a simple single-DOF analysis is adequate for most vibration isolation systems applied to stationary machines, it is insufficient to analyze a mechanism suspension to isolate higher frequency energy within vibrating screens. For most pieces of equipment, completely preventing all vibratory forces from being transmitted from a vibrating component to the surrounding structure would be ideal. But for a vibrating screen to function properly, the forces generated by the vibration mechanisms at their rotational speed must be transmitted to the body of the screen. Therefore, it is proposed to design a vibration mechanism suspension that transmits the vibration mechanism forces at their shaft speed while attenuating higher frequency force components due to bearing and gear vibrations.

There are several design considerations for an effective mechanism suspension. First, the tuned mechanism suspension cannot substantially decrease the response of the screen at the vibration mechanism operating frequency, because this would affect the ability of the screen to process coal. In addition, the vibration amplitude of the vibration mechanisms at the screen's operating speed cannot significantly increase, because this could decrease the life of the gears, bearings, drive belt, and drive motor. Since building vibration is a major concern, the mechanism suspension must not adversely affect the vibration transmitted to the building. Finally, the mechanism suspension

should reduce the force transmitted from the mechanisms to the screen body at frequencies where noise radiation is a concern. A target isolation frequency of 100 Hz was selected because most of the A-weighted sound power level is due to frequencies above 100 Hz.

3.1 Two-DOF Analysis of Screen with an Added Mechanism Suspension

The model shown in Fig. 3 was used to examine the dynamic characteristics of a screen with an added mechanism suspension while varying the spring rate for the mechanism suspension, k_j , from 8.755 MN/m to 17,510 MN/m. These values were used so that the system dynamics could be examined for a wide range of suspension stiffness with the hope of finding a range of stiffness values that would isolate operating forces at audible frequencies from the screen without creating problems due to suspension modes during startup, operation, and shutdown. The natural frequencies and mode shapes, the displacement responses for the vibration mechanisms and the screen body, the force transmitted from the vibration mechanisms to the screen body, and the force transmitted from the screen body to the ground were calculated for each spring rate.

Because the model has two degrees of freedom, there are two natural frequencies and mode shapes for the model. In the first mode, the vibration mechanisms and the screen body move in phase with the same amplitude. For the second mode, the vibration mechanisms and the screen body move out of phase with each other, and the amplitude of the vibration mechanisms is approximately seven times that of the screen body. Because the second mode gives the appearance of the vibration mechanisms bouncing on top of the screen body, this mode is referred to as a "bounce mode."

The two-DOF-analysis results showed that when the bounce mode was in the range of 50 to 70 Hz, the mechanism suspension attenuated the forces transmitted from the vibration mechanisms to the screen body above 100 Hz. In addition, the mechanism suspension did not significantly change the force transmitted from the vibration mechanisms to the screen body at the operating speed of the screen, 15 Hz. For subsequent analyses, the goal was to determine the mechanism suspension spring rates required to yield a bounce mode between 50 Hz and 70 Hz, without creating problems caused by pitching modes of the suspension.

The two-DOF analysis provided good insight into the behavior of the proposed suspension. Figures 8(a) and 8(b) show the response of the mechanisms and the

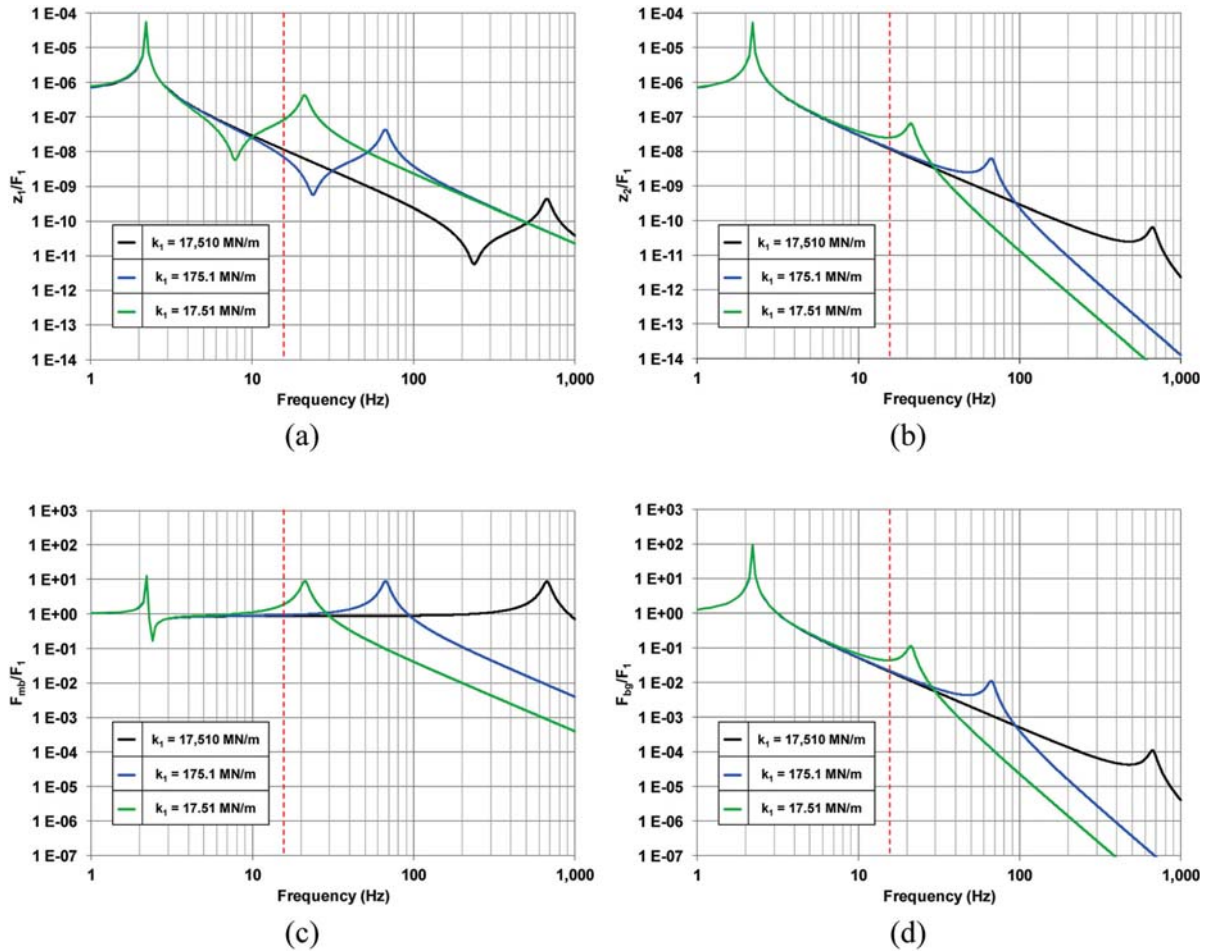
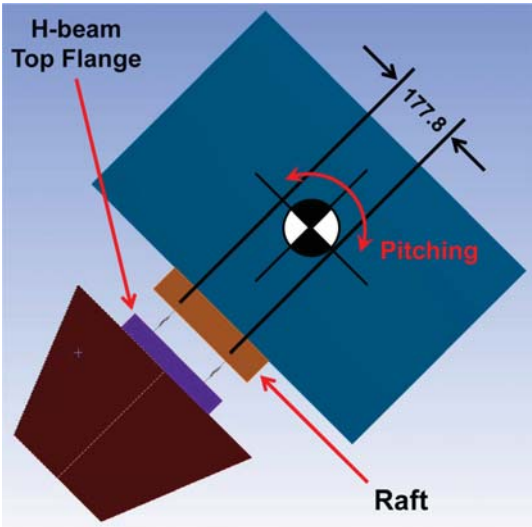


Fig. 8—System response per unit force based on a two DOF model using a unit load applied to the mechanisms: (a) response of the mechanisms; (b) response of the screen body; (c) force transmitted from the mechanisms to the screen body; and (d) force transmitted from the screen to the ground.

response of the screen body per unit force applied at the mechanisms. Figures 8(c) and 8(d) show the force transmitted from the mechanisms to the screen body and the force transmitted from the screen to the ground per unit force applied at the mechanisms. The red vertical line represents the operating speed of the vibration mechanisms, 15 Hz. Because the figures are based on a two DOF model, two resonant peaks occur. The lower resonant peak at approximately 2.1 Hz is not affected by the mechanism suspension spring rate. However, the frequency of the upper peak decreases with decreasing spring rate. In addition, the responses of both the screen body and the mechanisms at the operating speed are affected as the mechanism suspension spring rate is decreased. As the second resonant peak approaches the operating speed, the responses of the mechanisms and screen body at the operating speed are greatly amplified. As a result, both the force transmitted to the ground and the force transmitted to the screen body increase substantially.

3.2 FE Analysis of the As-Built Screen with an Added Mechanism Suspension

As in the two-DOF model, the frequency of the bounce mode for the FE model determines the frequency at which isolation of vibration mechanism forces begins. For the FE model, the bounce mode is identified by motion of the raft and the attached mechanisms normal to and out of phase with motion of the H-beam top flange. The bounce mode may also exhibit motion of other screen components. The mechanism suspension should have a bounce mode at roughly 50 to 70 Hz, because the two-DOF analysis showed that systems with mechanism suspension bounce modes in this range meet the design requirements discussed above. However, the spring rates from the two-DOF analysis provide only a rough starting point for the FE model, because adding a raft between the vibration mechanisms and the top flange of the H-beam in the FE model will increase the mass supported by the mechanism



Note: Dimensions in mm

Fig. 9—Side view of mechanism suspension, showing CG of mechanisms and mechanism suspension spring attachment points for the FE model of the as-built screen with added mechanism suspension.

suspension. This increase in sprung mass requires an increase in the mechanism suspension spring rates to keep the bounce mode in the range of 50 to 70 Hz.

Due to the geometry of the as-built screen, it was expected that achieving a mechanism suspension bounce mode of 50 to 70 Hz might result in a system with a pitch mode, with rotation about the lateral axis of the mechanism suspension, near or below the operating speed of the vibration mechanisms, 15 Hz. The top flange of the H-beam on the as-built screen is not very deep. This limited the spacing of the mechanism suspension mounting locations to 177.8 mm (refer to Fig. 9). In addition, the mechanisms are mounted so their centers of gravity are above their mounting surface. Both of these factors contribute to the presence of a pitch mode at low frequencies. The presence of a pitch mode near the operating speed could cause problems with the drive belt, bearings, gears, etc. If a pitch mode occurred below the operating speed, high amplitude motion during start-up and/or shutdown transients could be problematic.

To examine the modal characteristics of the as-built screen, the spring rates for each of the six mechanism suspension springs in the X_s -, Y_s -, and Z_s -directions (refer to Fig. 5) were varied from 44 MN/m to 17,510 MN/m. The 17,510-MN/m spring rate represents a rigid suspension, which would prevent relative motion between the raft and H-beam. The results, summarized in Table 1, showed that none of the spring rates resulted in a suspension that would meet the design objectives. For the rigid suspension, the pitch mode of the mechanisms involved twisting of the entire H-beam with no deflection of the springs, and the bounce mode did not exist because the spring rates were high enough to prevent relative motion between the raft and top flange of the H-beam. When the mechanisms suspension spring rates were 88 MN/m, the mechanism suspension bounce mode frequency was 73.5 Hz (refer to Fig. 10), just above the target range, and the mechanism suspension pitch mode frequency was 16.5 Hz (refer to Fig. 11). When the spring rates were 44 MN/m, the bounce mode frequency was 55.6 Hz and the pitch mode frequency decreased to 12.7 Hz. The suspensions with spring rates of 44 MN/m and 88 MN/m would probably cause problems due to the proximity of the pitch mode to the operating speed of the screen. To force the pitch mode well beyond the operating speed of the screen while keeping the bounce mode in the 50 to 70 Hz frequency range, the design of the mechanism suspension and the as-built screen must be modified.

3.3 Modal Analysis with FE Model of Screen with Increased Depth of H-beam Top Flange and Raft

In order to develop a successful mechanism suspension, the suspension's rotational stiffness about its y-axis must be increased to push the pitch mode far above the screen's operating speed. If this is done by increasing the mechanism suspension spring rates, the bounce mode of the suspension will be forced out of the 50 to 70 Hz range, and the resulting suspension will not begin to attenuate forces transmitted from the mechanisms to the screen body at 100 Hz. Therefore, instead of increasing the mechanism suspension spring rates, the distance between the suspension spring

Table 1—Summary of mechanism suspension spring rates and resulting pitch and bounce mode frequencies from modal analysis of the as-built screen with an added mechanism suspension.

Spring rate in X_s -, Y_s -, and Z_s -directions (MN/m)	17,510	88	44
F_{bounce} (Hz)	NA	73.5	55.6
F_{pitch} (Hz)	37.8	16.5	12.7

NA Not applicable

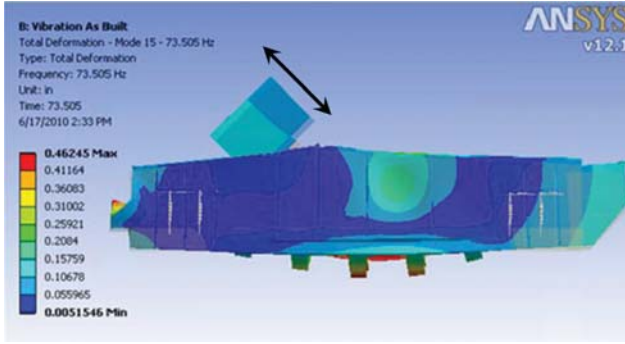


Fig. 10—Bounce mode of mechanism suspension for FE model of as-built screen with added mechanism suspension.

locations could be increased. This would also require the depth of the H-beam top flange and the depth of the raft to be increased.

For a simple system supported by linear springs that undergoes rotational motion about its center (refer to Fig. 12), the system's rotational stiffness is defined by

$$K_{rot} = \frac{k}{2}L^2 \quad (7)$$

where k is the spring rate and L is the distance between the springs. Because the rotational stiffness increases with the square of the distance between the springs, a small increase in the distance between the springs will significantly increase the rotational stiffness.

To improve the rotational stiffness for the mechanism suspension, the depth of the raft and the depth of the H-beam top flange were increased in the FE model, allowing the distance between the mechanism suspension springs to increase from 177.8 mm to 431.8 mm (refer to Fig. 13). From Eqn. (7), these changes increased the rotational stiffness of the mechanism suspension about its y-axis by a factor of 5.9. The changes

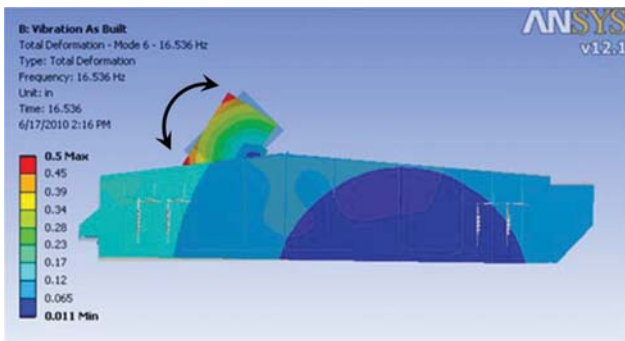


Fig. 11—Pitch mode of mechanism suspension for FE model of as-built screen with added mechanism suspension.

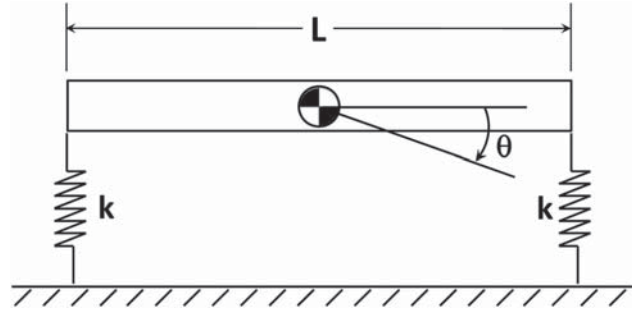


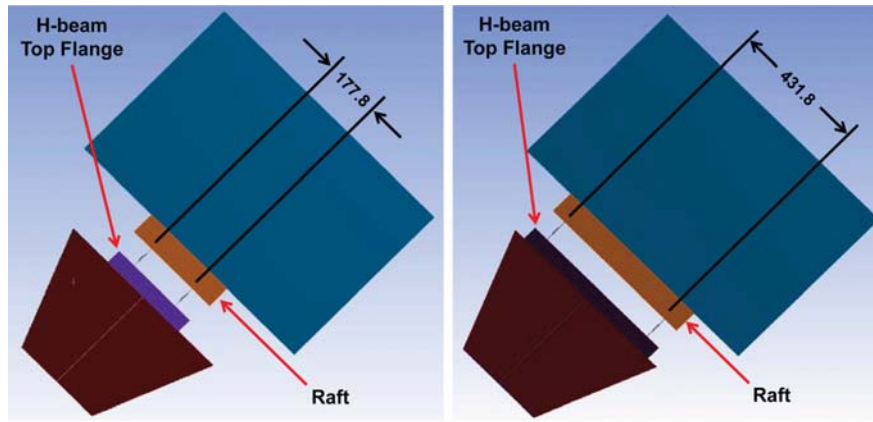
Fig. 12—A simple spring-supported system that undergoes rotational motion about its center.

to the raft also increased the mass of the raft and the mass of the H-beam top flange by a factor of 1.6. These changes increase the total mass of the screen by a small percentage.

As before, the FE model was used to perform modal analysis on the screen with the modified H-beam and raft for a variety of mechanism suspension spring rates. Table 2 summarizes the spring rates used and the resulting bounce and pitch mode frequencies. Case 1, which used a spring rate of 17,510 MN/m in all three directions, represents a rigid suspension. For the rigid case, a bounce mode was not observed, as expected. Case 2 used a spring rate of 175 MN/m in all three directions, and Case 3 used a spring rate of 35 MN/m in all three directions. Both of these cases yielded suspensions that met the target range of 50 to 70 Hz for the bounce mode. In addition, the pitch modes for each case were well above the operating speed of the screen. Some vibration isolation mounts are much stiffer in off-axis directions. Case 4, which uses the same spring rate as Case 3 in the Z_s -direction and spring rates that are five times higher in the X_s - and Y_s -directions, was used to examine how these conditions would affect the modes. As Table 2 shows, the large increases in the stiffness in the X_s - and Y_s -directions (Case 4) had a minimal effect on the frequencies of the pitch and bounce modes.

3.4 Forced Response Analysis and Estimation of Sound Power Level

After providing a good understanding of how the frequencies of the pitch and bounce modes change with the mechanism suspension spring rates, the FE model was used to perform a forced response analysis for a range of mechanism suspension spring rates using the modal superposition method. Table 3 summarizes the mechanism suspension spring rates used in the analysis. Case A, which uses a spring rate of 17,510 MN/M in all three directions, represents a rigid



Note: Dimensions in mm

Fig. 13—Comparison of mechanism suspension spring spacing along the depth of the H-beam for the model of the as-built screen (left) and for the model of the screen with increased H-beam top flange and raft depth (right).

connection. Case B, which uses a spring rate of 175 MN/m in the Z_s -direction, has a bounce mode of approximately 67 Hz. Case C uses a spring rate of 35 MN/m in the Z_s -direction, which yields a bounce mode of 50 Hz. For Cases B and C, the spring rates in the X_s - and Y_s -directions were five times their respective spring rates in the Z_s -direction. The spring rates for Case B and Case C were selected because they produce systems with bounce mode frequencies at the extremes of the desired target range for the bounce mode.

Several assumptions were made to simplify the model and to enable the use of the modal superposition technique. In the analysis, the spring rates were considered to have a fixed value as a function of frequency. In addition, a constant modal damping of 0.002 was used for all modes. This value was used because previously collected experimental modal data showed that the as-built screen is lightly damped. In practice, rubber vibration isolators would probably be used for the mechanism suspension. For rubber vibration isolators, the stiffness and damping increase as a function of frequency. As a result, the FE model will tend to underes-

timate the displacements at high frequencies. However, assuming constant values allows trends to be observed while allowing modal superposition to be used to solve the problem instead of explicitly solving for the response. Due to the large model size, the explicit solution would require significantly more solution time and computational power.

In the analysis, a unit load with a flat input spectrum from 0 to 500 Hz was applied to the raft at the center of each mechanism. These loads represent the impact forces generated by the interaction of the eccentric shafts with the bearings. Clearance in the bearings allows the vibration mechanism shafts to make and break contact with the bearing's rolling elements as the screen vibrates. It is likely that the real force spectrum is not flat. However, for comparison purposes, assuming a flat input spectrum should be adequate. It is expected that the actual force spectrum would roll off at higher frequencies similar to the spectrum of an impact hammer used for modal testing.

The mechanism suspensions with bounce modes in the 50 to 70 Hz frequency range, Case B and Case C,

Table 2—Mechanism suspension spring rates and resulting pitch and bounce mode frequencies for the modal analysis of the screen with added mechanism suspension and increased H-beam top flange and raft depth.

Mechanism Suspension Spring Rates (MN/m)	Direction	Case 1	Case 2	Case 3	Case 4
	X_s	17,510	175	35	175
	Y_s	17,510	175	35	175
	Z_s	17,510	175	35	35
F_{pitch} (Hz)		54	37.7	23.4	24.0
F_{bounce} (Hz)		NA	67.1	50.1	50.2

NA Not applicable

Table 3—Mechanism suspension spring rates for the forced response analysis of the screen with added mechanism suspension and increased H-beam top flange and raft depth.

	Direction	Case A	Case B	Case C
Mechanism Suspension Spring Rates (MN/m)	X_s	17,510	876	175
	Y_s	17,510	876	175
	Z_s	17,510	175	35

reduced the estimated sound power level in the 0 to 500 Hz frequency range. Figure 14 shows the estimated A-weighted sound power level from the screen sides and feedbox in 1/3-octave bands as computed from Eqn. (4). Case A represents the baseline because its response should be similar to that of a screen with its mechanisms bolted directly to the H-beam. For Case A, the spectrum exhibits a hump in the 250 Hz through 500 Hz 1/3-octave bands. The measured sound power level, shown in Fig. 2, also exhibits this characteristic. Recall, the results presented in Fig. 14 are based on a unit force with a flat input spectrum applied at the center of each mechanism. The real forces applied to the mechanisms by the bearings will probably not have flat spectra. Instead, the real input forces would probably exhibit peaks near the bearing frequencies. Therefore, the results should only be used to examine trends.

The suspensions for Case B and Case C shift the sound power level spectrum towards lower frequencies. The figure shows that the estimated overall A-weighted sound power level from 0 to 500 Hz is 74 dB for Case A, 67 dB for Case B, and 56 dB for Case C. Treating Case A as the baseline (mechanisms rigidly

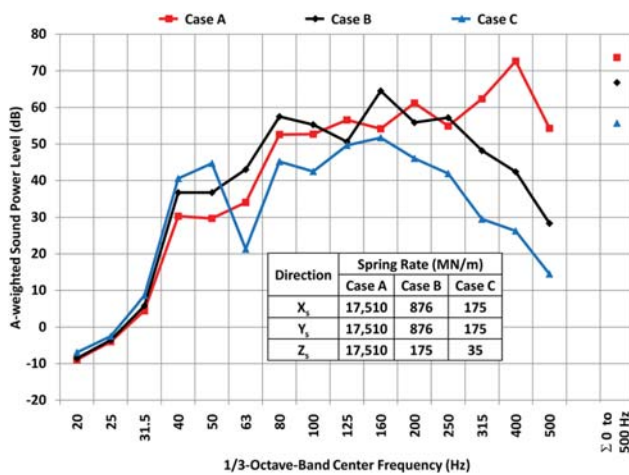


Fig. 14—Estimated A-weighted sound power level in 1/3-octave bands for two mechanism suspensions compared to a rigid mechanism suspension.

connected), Case B and Case C reduced the estimated A-weighted sound power level by 7 dB and 18 dB, respectively. In a real world application of these mechanism suspensions, it is unlikely that the sound power level would be reduced by these values. However, the results show how mechanism suspensions could reduce the A-weighted sound power level.

With the previously discussed assumptions, the results indicate that the sound power level radiated by the screen sides and feedbox decreases as the mechanism suspension spring rate normal to the H-beam is adjusted to produce mechanism suspension bounce modes in the 50 to 70 Hz frequency range. In practice, the screen and mechanism suspension designs must be modified to ensure that other modes of vibration, such as the mechanism suspension pitch mode, occur at frequencies well beyond the operating speed of the screen. Another factor to consider is that the magnitude of the impact forces generated within the vibration mechanisms might be affected by the mechanism suspension stiffness. If the displacement of the vibration mechanism housings increases above the baseline value, the forces due to bearing slap will probably increase. If the increase in the bearing slap forces is equal to the attenuation in the force transmitted, the net result will be that the sound power level will stay the same. It is also possible that the increase in bearing slap forces could exceed the attenuation provided by a mechanism suspension system. In this case, the sound power level would increase. As demonstrated, caution must be exercised when implementing a mechanism suspension system. A slightly stiffer system could ultimately yield a larger reduction in sound power level than a softer system.

4 CONCLUSIONS

The addition of a mechanism suspension to a vibrating screen was analyzed using a simple two-DOF model and an FE model. The two-DOF analysis showed that mechanism suspensions with bounce modes from 50 to 70 Hz could transmit vibration at the screen's operating speed while attenuating vibration at frequencies above 100 Hz. For the as-built screen with

an added mechanism suspension, FE modal analysis showed that a mechanism suspension pitch mode would occur close to the screen's operating speed for mechanism suspensions with bounce modes from 50 to 70 Hz. These systems might successfully attenuate noise and vibration above 100 Hz, but because their pitch modes would be close to the screen's operating speed, these systems could cause undesirable behavior during screen start-up, shutdown, and steady operation. In the FE model, changes were made to the H-beam and the mechanism suspension to increase the rotational stiffness of the suspension to force the pitch mode to higher frequencies. Increasing the depth of the H-beam top flange and the depth of the raft allowed the spacing between the suspension springs to be increased. For mechanism suspensions with bounce modes of 50 to 70 Hz, this shifted the mechanism suspension pitch mode to higher frequencies.

The modified FE model was used to estimate the sound power level radiated by the screen sides and feedbox due to a unit force applied at the center of each vibration mechanism. The estimated sound power levels for mechanism suspensions with bounce modes of 50 and 67 Hz were compared to those of a rigid suspension. The estimated A-weighted sound power level from the screen sides and feedbox was reduced by 7 to 18 dB, depending on the mechanism suspension stiffness. It is important to realize that this analysis only considers noise radiated by the screen sides and feedbox due to gear and bearing forces within the vibration mechanisms. In reality, vibrating screen noise is generated from many components. In addition, because these results are based on several assumptions, these reductions would probably not be achieved in practice. However, even though the FE model was simplified by assuming non-frequency-dependent spring rates, constant modal damping, and flat force spectra, the analysis shows that a mechanism suspension could be designed to reduce vibration-related screen noise due to high frequency forces within the vibration mechanisms.

The analysis revealed several important factors to consider in the design of a mechanism suspension for vibrating screens. First, to attenuate noise at frequencies above 100 Hz without significantly affecting a screen's performance, the bounce mode of the screen suspension must be kept within the range of 50 to 70 Hz. Next, the spacing between the vibration isolation mount locations must be increased to force the suspension pitch mode to

higher frequencies where it will not be well-excited during screen start-up, shutdown, or operation. The analysis used here showed that a suspension system with a 50 Hz bounce mode would reduce noise more than a system with a 70 Hz bounce mode. While the results indicate that adding a mechanism suspension to a screen will significantly decrease radiated noise, these results must be verified experimentally. The next phase of this research will consist of adding a mechanism suspension to a vibrating screen and measuring the resulting sound power levels.

5 REFERENCES

1. Department of Labor, Mine Safety and Health Administration, "Health Standards for Occupational Noise Exposure: Final Rule," 30 CFR Part 62. *Federal Register*, (1999).
2. E. R. Bauer, Personal communication. DHHS, CDC, NIOSH, PRL, Pittsburgh, PA, (2004).
3. Mine Safety and Health Administration. <http://www.msha.gov/OpenGovernmentData/OGIMSHA.asp> downloaded December 9, 2010 with the exception of the MSHA Accident data file, which was added December 27, 2010.
4. E. E. Ungar, G. E. Fax, W. N. Patterson and H. L. Fox, "Coal Cleaning Plant Noise and Its Control", BuMines OFR 44-74, (1974).
5. M. N. Rubin, A. R. Thompson, R. K., Cleworth and R. F. Olson, "Noise Control Techniques for the Design of Coal Preparation Plants", BuMines OFR 42-84, (1982).
6. D. S. Yantek, P. Jurovcik and E. R. Bauer, "Noise and Vibration Reduction of a Vibrating Screen", *SME Annual Meeting, Society for Mining, Metallurgy, and Exploration*, (2005).
7. D. S. Yantek, H. E. Camargo and R. J. Matetic, "Application of a microphone phased array to identify noise sources on a horizontal vibrating screen", *NoiseCon08*, (2008).
8. H. E. Camargo, P. A. Ravetta, R. A. Burdisso and D. S. Yantek, "Noise source identification on a horizontal vibrating screen", *Mining Engineering*, (2009).
9. D. S. Yantek and H. E. Camargo, "Structural vibration as a noise source on vibrating screens", *ASME 2009 International Mechanical Engineering Congress & Exposition*, (2009).
10. M. J. Lowe, D. S. Yantek, H. E. Camargo, L. A. Alcorn and M. Shields, "Noise controls for vibrating screen mechanisms", *SME Annual Meeting, Society for Mining, Metallurgy, and Exploration, Inc.*, (2010).
11. D. S. Yantek and S. Catlin, "Evaluation of stiffeners for reducing noise from horizontal vibrating screens", *NoiseCon10*, (2010).
12. E. E. Ungar, C. L. Dym, and M. H. Rubin, "Practical Reduction of Noise from Chutes and Screens in Coal Cleaning Plants", BuMines OFR 59-77, (1976).
13. Singeresu S. Rao, "Two degree of freedom systems", Chap. 5 in *Mechanical Vibrations – Second Edition.*, Addison Wesley Publishing Company, Inc., (1990).
14. D. A. Bies and C. H. Hansen, *Engineering Noise Control Theory and Practice*. Third Edition. Spon Press, (2003).